

Determination of the fermion pair size in a resonantly interacting superfluid

Christian H. Schunck¹, Yong-il Shin¹, André Schirotzek¹ & Wolfgang Ketterle¹

Fermionic superfluidity requires the formation of particle pairs, the size of which varies from the femtometre scale in neutron stars and nuclei to the micrometre scale in conventional superconductors. Many properties of the superfluid depend on the pair size relative to the interparticle spacing. This is expressed in ‘BCS–BEC crossover’ theories^{1–3}, describing the crossover from a Bardeen–Cooper–Schrieffer (BCS)-type superfluid of loosely bound, large Cooper pairs to Bose–Einstein condensates (BECs) of tightly bound molecules. Such a crossover superfluid has been realized in ultracold atomic gases where high-temperature superfluidity has been observed^{4,5}. The microscopic properties of the fermion pairs can be probed using radio-frequency spectroscopy. However, previous work^{6–8} was difficult to interpret owing to strong final-state interactions that were not well understood. Here we realize a superfluid spin mixture in which such interactions have negligible influence and present fermion pair dissociation spectra that reveal the underlying pairing correlations. This allows us to determine that the spectroscopic pair size in the resonantly interacting gas is 20 per cent smaller than the interparticle spacing. These are the smallest pairs so far observed in fermionic superfluids, highlighting the importance of small fermion pairs for superfluidity at high critical temperatures⁹. We have also identified transitions from fermion pairs to bound molecular states and to many-body bound states in the case of strong final-state interactions.

The properties of pairs are revealed in a dissociation spectrum, where pair dissociation is monitored as a function of the applied energy E . The spectrum has a sharp onset at the pair’s binding energy E_b , where the fragments have zero kinetic energy, and then spreads out at higher energies. Because a radio-frequency photon has negligible momentum, the allowed momenta for the fragments reflect the Fourier transform $\Phi(k)$ of the pair wavefunction $\phi(r)$, which has a width on the order of $1/\xi$, where ξ is the pair size. Thus, the pair size can be estimated from the spectral linewidth E_w as $\xi^2 \approx \hbar^2/mE_w$, where m is the mass of the particles and \hbar is Planck’s constant h divided by 2π .

The conceptually simplest pairs in the BCS–BEC crossover are the weakly bound molecules in the BEC limit, which are described by a spatial wavefunction $\phi_m(r) \propto e^{-r/b}/r$ with a binding energy $E_b = \hbar^2/mb^2$ and a root-mean-square size of $b/\sqrt{2}$. When the molecules are dissociated into non-interacting free particles, the spectral response is $I_m \propto \sqrt{E - E_b}/E^2$, which shows a highly asymmetric line shape with a steep rise at the molecular binding energy E_b and a long ‘tail’ at higher energies^{5,10} (Fig. 1a).

This general behaviour of the dissociation spectrum also holds in the BCS limit, where pairing is a many-body effect^{5,11}. The radio-frequency dissociation process discussed below, in the limit of negligible final-state interactions, can be considered as breaking a Cooper pair into one quasi-particle and one free particle. The radio-frequency spectrum in the BCS limit¹² has an onset at $\Delta^2/2E_F$ and the same $E^{-3/2}$

energy dependence at high energy as in the BEC limit (Fig. 1b; here E_F is the Fermi energy and Δ is the gap). Because the radio-frequency excitation occurs throughout the whole Fermi sea, it is most natural to interpret the BCS state as $N/2$ pairs with condensation energy $\Delta^2/2E_F$, where N is the total number of fermions⁵.

A spectroscopic pair size can be defined from either the onset or the width of the radio-frequency spectrum as $\xi_{th}^2 = \hbar^2/2mE_{th}$ or, respectively, $\xi_w^2 = \gamma \hbar^2/2mE_w$. Here E_{th} is the onset/threshold energy, E_w is the full width at half maximum and $\gamma = 1.89$ is a numerical constant chosen for convenience (see Fig. 1 legend). The pair sizes ξ_{th} and ξ_w , which can be directly obtained from the radio-frequency spectrum, capture the evolution of the pair size from the BCS limit to the BEC limit (Fig. 1c).

Because the radio-frequency spectra have similar behaviour in both limiting cases of the BCS–BEC crossover, we would expect comparable spectra within the crossover regime. Surprisingly, the radio-frequency spectra obtained in previous radio-frequency experiments did not fit into this picture: the line shape did not show any pronounced asymmetry and the linewidth was narrow^{6–8} (Supplementary Fig. 3). These experiments could therefore not be simply interpreted in terms of pairing energy and pair size. We will show that this is caused by strong final-state interactions and transitions to bound states.

In both the previous experiments and our new ones, the fermion pairs consist of two atoms in different hyperfine states $|a\rangle$ and $|b\rangle$. The radio-frequency pulse transfers atoms in state $|b\rangle$ to an initially unoccupied third state $|c\rangle$. In addition to pair dissociation, also referred to as a ‘bound–free’ transition and characterized by the asymmetric line shape discussed above, radio-frequency spectroscopy can induce a second kind of transition to another bound state, that is, the transfer of a pair (a, b) to a pair (a, c) (also referred to as a ‘bound–bound’ transition). The latter spectra have narrow, symmetric line shapes.

Final-state effects arise when the dissociated atom in state $|c\rangle$ interacts with atoms in state $|a\rangle$. The interaction strength is measured by the dimensionless parameter $k_F a$. Here a is the s -wave scattering length; we use a_i and a_f to denote these lengths in the initial (a, b) and, respectively, final (a, c) interactions. As discussed in detail below, final-state interactions strongly affect the radio-frequency dissociation spectra^{13–15} when $|k_F a_f| > 1$. To overcome this problem, it is necessary to change the interactions in the final state without changing those in the initial state. Our solution is the realization of a new high-temperature superfluid in ⁶Li using a different combination of hyperfine states for which radio-frequency excitation with reduced final-state interactions is possible (see Methods). As a result, we were able to resolve the bound–bound and bound–free contributions to the radio-frequency spectrum, and to determine the size of fermion pairs from the asymmetric fermion pair dissociation spectra.

We have taken advantage of the fact that any two-state mixture, (1, 2), (1, 3) or (2, 3), of the three lowest hyperfine states of ⁶Li

¹Department of Physics, MIT–Harvard Center for Ultracold Atoms, and Research Laboratory of Electronics, MIT, Cambridge, Massachusetts 02139, USA.

(labelled in the order of increasing hyperfine energy as $|1\rangle$, $|2\rangle$ and $|3\rangle$) exhibits a broad s -wave Feshbach resonance^{16,17}. So far, all experiments with strongly interacting fermions in ^6Li have been carried out in the vicinity of the (1, 2) Feshbach resonance located at $B_{12} \approx 834$ G (B_{ij} denotes the centre of the broad s -wave Feshbach resonance in the (i, j) mixture). Surprisingly, inelastic collisions including allowed dipolar relaxation are not enhanced by the (1, 3) and (2, 3) Feshbach resonances. We observe that at both the (1, 3) and (2, 3) Feshbach resonances, superfluids can be created as well (see Methods). This doubles the number of high-temperature superfluids available for experimental studies.

The newly created (1, 3) superfluid is the best choice for radio-frequency spectroscopy experiments because the final-state scattering length a_f at the (1, 3) resonance position $B_{13} \approx 691$ G is small and positive ($0 < k_F a_f < 1$ for typical values of k_F). Therefore the accessible final states are either a molecule of well-defined binding energy

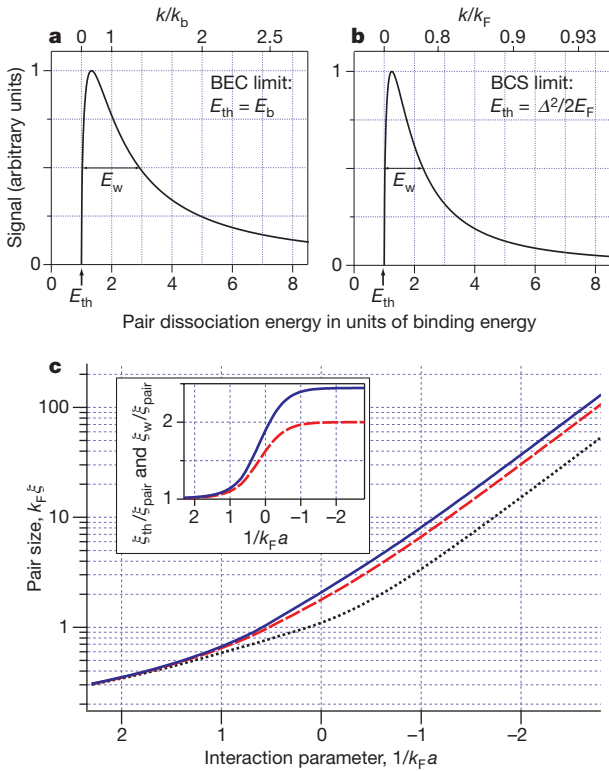


Figure 1 | Line shape of the pair dissociation spectrum in the BEC and BCS limits and the evolution of the fermion pair size in the BCS-BEC crossover^{5,11,20}. **a, b**, Simulated radio-frequency dissociation spectra in the BEC (**a**) and BCS (**b**) limits. The momentum k of the free particles after dissociation is indicated in the top axes, where $\hbar^2 k_b^2/m = E_b$ and k_F is the Fermi wavenumber. Apart from an offset, the spectra in the BEC and BCS limits have almost indistinguishable line shapes. The molecular dissociation line shape I_m with an additional offset parameter can therefore serve as a generic, model-independent fitting function for pair dissociation spectra (see Methods and Supplementary Fig. 2). **c**, The fermion pair sizes ξ_w (solid blue) and ξ_{th} (dashed red) are displayed as a function of the interaction parameter $1/k_F a$. Also shown is the two-particle correlation length ξ_{pair} (dotted black), given by $\xi_{pair} = \sqrt{\langle \phi | r^2 | \phi \rangle / \langle \phi | \phi \rangle}$, where $\phi(r) = \langle \psi | \Psi_{\alpha}^{\dagger}(r) \Psi_{\beta}^{\dagger}(0) | \psi \rangle$. Here ψ is the generalized BCS wavefunction and α and β refer to the two components². In the BEC limit, the value for the molecular size is $\xi_m = b/\sqrt{2} = \xi_{pair}$ and we choose $\gamma = 1.89$ in the definition of ξ_w , so $\xi_m = \xi_{th} = \xi_w$. In the BCS limit, $\xi_{pair} = (\pi/2\sqrt{2})\xi_c$, where $\xi_c = \hbar^2 k_F / \pi m \Delta$ is the Pippard coherence length, and we have $\xi_{th} = 2\xi_{pair}$ and $\xi_w = 2.44\xi_{pair}$. The inset shows the ratios ξ_w/ξ_{pair} (solid blue) and ξ_{th}/ξ_{pair} (dashed red). Although ξ_{pair} changes by orders of magnitude, ξ_{th} and ξ_w show the same behaviour as ξ_{pair} , deviating from each other by not more than 22%. This illustrates that the pair size can be reliably determined from the radio-frequency dissociation spectrum throughout the whole BCS-BEC crossover.

or two free, only weakly interacting atoms. The actual final-state interactions depend on whether we drive the radio-frequency transitions from $|1\rangle$ to $|2\rangle$ or from $|3\rangle$ to $|2\rangle$, allowing the comparison of spectra taken from the same sample but with different a_f values (see Methods and Supplementary Information). After preparing the (1, 3) superfluid, a radio-frequency pulse resonant with the $|3\rangle$ -to- $|2\rangle$ transition is applied. Then either the losses in state $|3\rangle$ or the atoms transferred to state $|2\rangle$ are monitored (see Methods). All spectra are plotted versus frequency or energy relative to the atomic resonance, that is, relative to the energy E_0 required to transfer an atom from $|3\rangle$ to $|2\rangle$ in the absence of atoms from state $|1\rangle$.

The main results of this paper are the spectra observed in the (1, 3) BEC-to-BCS crossover between 670 and 710 G (Fig. 2). The spectra have the asymmetric shape characteristic of pair dissociation and are indeed well fit by a generic pair dissociation line shape convolved with the line shape of the square excitation pulse (see Fig. 1 and Methods). If the frequency axis is scaled by E_w and the spectra are shifted to show the same onset, all three spectra overlap as shown in Fig. 3a. At the level of our experimental resolution, the dissociation line shape is therefore not sensitive to the change in interactions. As illustrated in Fig. 1, the pair size can in principle be obtained from both E_{th} and E_w . However, because the whole spectrum may be subject to shifts due to Hartree terms^{16,18}, in the following we focus only on the width of the spectrum.

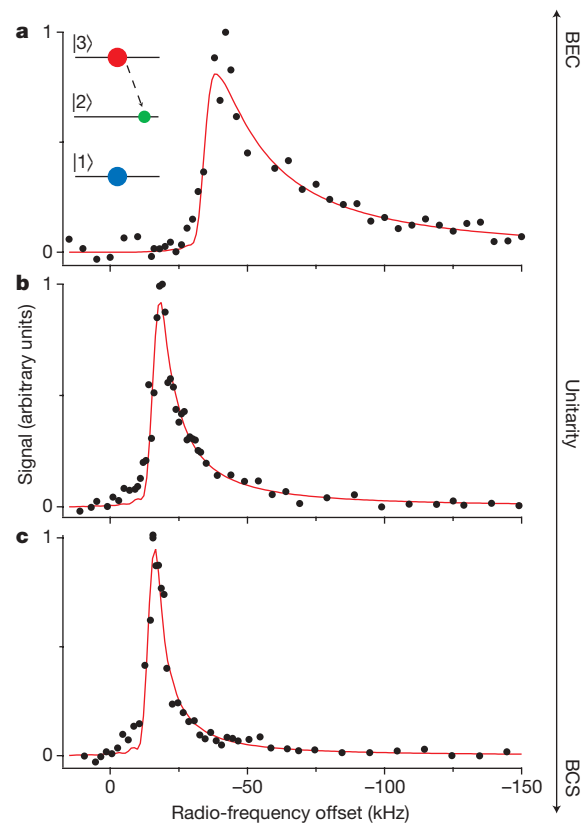


Figure 2 | Radio-frequency dissociation spectra in the BCS-BEC crossover. Below (**a**), at (**b**) and above (**c**) resonance, the spectrum shows the typical asymmetric shape of a pair dissociation spectrum. The signal is proportional to the three-dimensional local response at the centre of the cloud (see Methods). The red traces are fits to the spectra. Because state $|3\rangle$ has a higher energy than state $|2\rangle$ (see the inset in **a**), the dissociation energy is always less than the transition frequency E_0/\hbar for the atomic resonance, and the dissociation spectra therefore appear at energies that are negative relative to E_0 . The inverted frequency axis ensures that the dissociation spectrum is always on the right-hand (or ‘positive’) side of the origin. The magnetic fields, the local Fermi energies ϵ_F , the temperatures and the interaction strengths $1/k_F a_i$ are 670 G, $\hbar \times (24 \text{ kHz})$, $\sim 0.2 T_F$, 0.4 (**a**); 691 G, $\hbar \times (21 \text{ kHz})$, $0.1 T_F$, ~ 0 (**b**); 710 G, $\hbar \times (17 \text{ kHz})$, $0.1 T_F$, -0.3 (**c**).

At unitarity we determine the full width at half maximum to be $E_w = 0.28(5)\varepsilon_F$, corresponding to a spectroscopic pair size $\xi_w = 2.6(2)/k_F$ (here ε_F is the local Fermi energy and $k_F = \sqrt{2m\varepsilon_F}/\hbar$; the quoted errors are purely statistical). The pairs are therefore smaller than the interparticle spacing l , given by $l = n^{-1/3} = (3\pi^2)^{1/3}/k_F \approx 3.1/k_F$ (where n is the total density), and in units of $1/k_F$ are the smallest reported so far for fermionic superfluids. In high-temperature superconductors, ξ values at optimal doping are in the range $5/k_F$ – $10/k_F$ (ref. 9).

In the simple BEC-to-BCS crossover model, the ratio ξ_{pair}/ξ_w varies from 1 to about 0.4. The fact that ξ_w is smaller than the interparticle spacing suggests the use of the molecular ratio, that is, $\xi \equiv \xi_{\text{pair}} = \xi_w = 2.6/k_F$. Before we compare this result with theoretical predictions, we note that various definitions of the pair size differ by factors on the order of unity¹⁹. With this in mind, we find that the ξ value we observe is larger than the pair size of about $1/k_F$ predicted from a functional integral formulation of the BCS–BEC crossover²⁰. Small fermion pair sizes have been explicitly linked to high critical temperatures (T_c) through the relation $T_c/T_F \approx 0.4/k_F\xi_{\text{pair}}$ (where T_F is the local Fermi temperature), which applies for weak coupling⁹. Inserting the observed ξ value into this relation yields an estimate of $T_c/T_F \approx 0.15$, which lies in the predicted range of values, 0.15 to 0.23 (ref. 21). If we use the asymptotic BCS relation $\Delta = (\hbar^2/\pi m)(k_F/\xi_c) = (\varepsilon_F/\sqrt{2})(1/k_F\xi_{\text{pair}})$, which is valid at weak coupling, and our observed value of ξ at unitarity, we find that $\Delta \approx 0.3\varepsilon_F$, which is smaller than the value of $0.5\varepsilon_F$ predicted by Monte Carlo simulations²².

The strong narrowing of the spectral line in Fig. 2a–c demonstrates that the fermion pair size increases from strong to weak coupling. The decreasing width corresponds to a more than twofold increase of the spectroscopic pair size, from $\xi_w = 1.4(1)k_F$ at 670 G to $\xi_w = 3.6(3)k_F$ at 710 G. A change in the absolute pair size with density at unitarity can in principle be observed by comparing the spectral width in the centre with that in the outer regions of the trapped cloud. As the density decreases, the spectrum shifts to lower energies (Fig. 3b). However, the spectral onset also becomes increasingly softer and

the asymmetry of the pair dissociation peak less pronounced, possibly because of atomic diffusion during the excitation pulse. This prevents a reliable determination of the pair size in the spatial wings, where the density is changing rapidly.

We now consider the effect of final-state interactions in more detail. First we would like to point out that the increase in a_f by a factor of about two between 670 G and 710 G has not affected the spectra in Fig. 3a, within the experimental resolution. This suggests that final-state effects are small for these spectra. Additional information is obtained from the previously introduced bound–bound transitions, which lie outside the range plotted in Fig. 2. On the BEC side of the resonance, the (1, 3) molecule can be transferred also to a more deeply bound (1, 2) molecule (Fig. 4a). The bound–bound peak is still present at unitarity and also on the BCS side at 710 G (Fig. 4b and c), and results from the transition of a many-body bound fermion pair to a (1, 2) molecule. The strong overlap of the pair wavefunction and the molecule in the final state is another indication of the ‘molecular’ character of the fermion pairs in the strongly interacting regime.

The spectra start to change significantly at higher magnetic field. As the magnetic field is increased, the (1, 3) mixture remains in the unitarity-limited regime, with the interaction strength approaching $1/|k_F a_f| \approx 1$ at B_{12} . The final-state interactions, however, change from weak to strong, causing the pair dissociation peak to decrease in weight and the bound–bound peak to become dominant (Fig. 4d–f). This single peak apparently corresponds to a bound–bound transition from many-body bound (1, 3) pairs to the highly correlated final state of an atom in $|2\rangle$ interacting with the paired atoms in $|1\rangle$.

A narrow bound–bound peak is predicted both in the molecular (two-body) and the many-body case, when initial- and final-state interactions are identical or similar. The spectra in Fig. 4 show that bound–bound transitions dominate when $|1/k_F a_i - 1/k_F a_f| \leq 1.5$. In our opinion, a recent theoretical treatment (ref. 23 and S. Basu and E. J. Mueller, personal communication) agrees qualitatively with these results but underestimates the extent of the region in which bound–bound transitions are dominant by a factor of about two. Our observations allow a reinterpretation of the radio-frequency spectra obtained from the (1, 2) superfluid with resonant interactions^{6–8} (see the Supplementary Information for an extended discussion). The spectra have been taken in the regime $|1/k_F a_i - 1/k_F a_f| \leq 1$, where strong bound–bound transitions are expected. Together with the very narrow and symmetric line shape (Supplementary Fig. 3), this suggests that the (1, 2)-to-(1, 3) radio-frequency spectra at 833 G are dominated by such bound–bound transitions and cannot be simply interpreted in terms of a pair dissociation process and a pairing gap^{6–8,24–26}.

In conclusion, we have determined the pair size of resonantly interacting fermions using new superfluid spin mixtures in ${}^6\text{Li}$. The (1, 3) mixture is ideally suited to radio-frequency spectroscopy because final-state interactions do not significantly affect the spectra. Our measurements clearly reveal the microscopic structure of the fermion pairs in the strongly interacting regime. The small fermion pair size and high critical temperatures that we observe in our system show an interrelationship similar to the one suggested by the Uemura plot for a wide class of fermionic superfluids⁹. Our results also explain why the rapid-ramp method used to observe fermion pair condensation in the crossover has been successful^{27,28}. The small pair size facilitated the efficient transfer of the many-body bound fermion pairs to more strongly bound molecules, while preserving the momentum distribution of the pairs.

This work presents several opportunities for future research. The microscopic structure of the pairs can now be studied both in the superfluid and normal phase as a function of interaction strength, temperature and spin imbalance between the two components⁷. Increased spectral resolution may reveal interesting deviations of the spectral shape from the generic line shape discussed here.

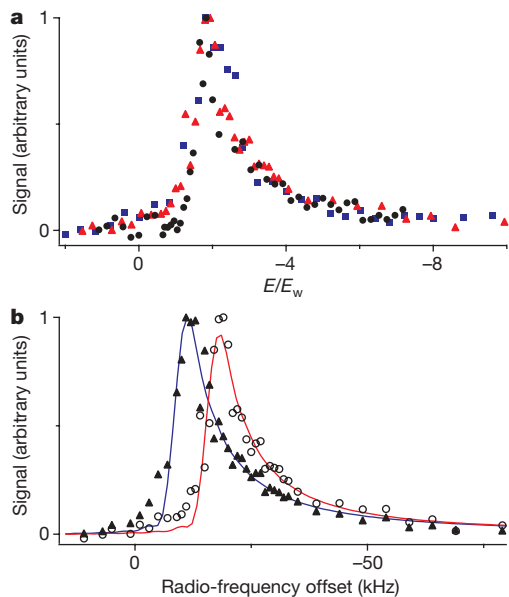


Figure 3 | Comparison of line shapes and density effects. a, Same spectra as in Fig. 2 but with the frequency axis scaled by E_w and shifted so that the spectral onset overlaps with the BEC-side spectrum: black circles, BEC side; red triangles, resonance; blue squares, BCS side. **b**, Density effects at unitarity. The figure shows the tomographically reconstructed spectral response in the centre (open circles, same spectrum as in Fig. 2b; fit by red trace) as well as the lower-density wings (filled triangles; fit by blue trace) of the cloud. In this regime the cloud might be in the normal (as opposed to superfluid) phase.

Furthermore, the predicted universality of a resonantly interacting Fermi mixture can now be tested in ${}^6\text{Li}$ in three different systems. The lifetimes of all three two-state combinations of the three lowest

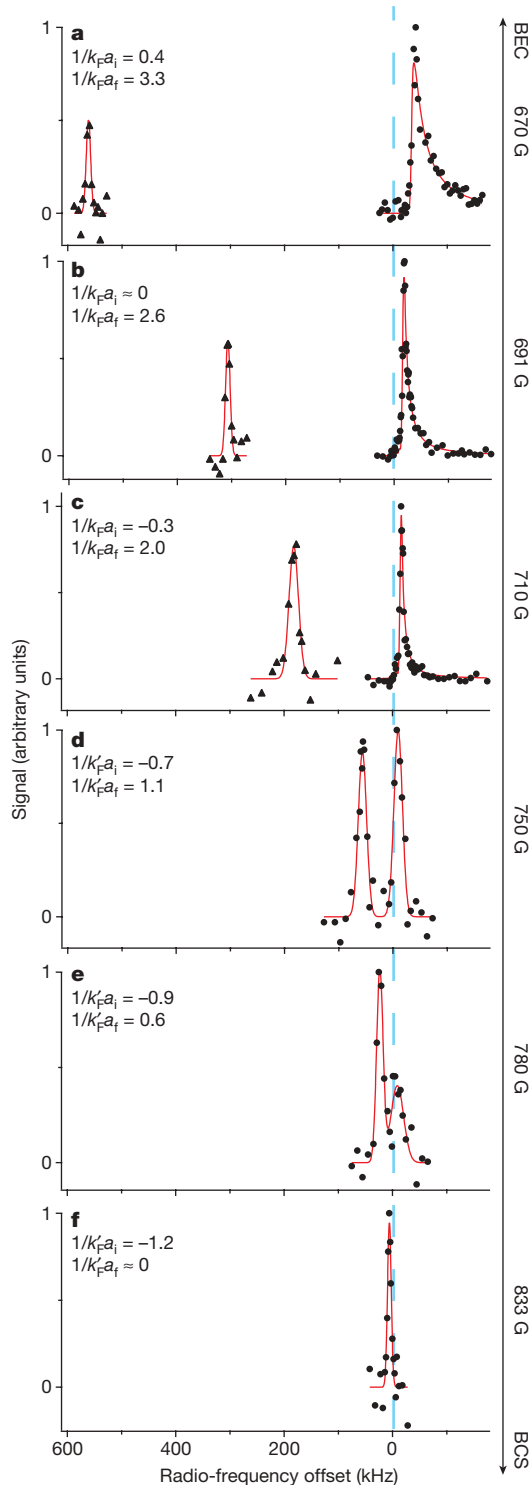


Figure 4 | Effect of final-state interactions on radio-frequency spectroscopy: bound-bound and bound-free spectra in the BCS–BEC crossover of the (1, 3) mixture. Although the initial (1, 3) state is strongly interacting at all fields, the final-state interactions change from weak (a–c) to strong (d–f). See ref. 17 for a plot of the Feshbach resonances. At the higher magnetic fields for $1/k_F a_i \approx -1$, the initial state might be in the normal phase. a–c, Same bound–free spectra and parameters as in Fig. 2. The relative weight of the bound–bound and bound–free peaks could not be determined experimentally (see Methods). d, 750 G, $E_F = h \times (22 \text{ kHz})$, $T/T_F = 0.09$; e, 780 G, $E_F = h \times (23 \text{ kHz})$, $T/T_F = 0.09$; f, 833 G, $E_F = h \times (20 \text{ kHz})$, $T/T_F = 0.06$.

hyperfine states in ${}^6\text{Li}$ are on the order of 10 s in the strongly interacting regime. The three-body decay rates, however, decrease by more than an order of magnitude between 690 and 830 G for a ternary mixture, which may reflect interesting three-body physics. The longer lifetime of 30 ms at 691 G might be sufficient for studies involving all three hyperfine states²⁹, with the potential for experiments on pairing competition in multi-component Fermi gases and spinor Fermi superfluids.

METHODS SUMMARY

Creation of the (1, 3) superfluid. By a method described previously⁵, a spin-polarized sample of ultracold ${}^6\text{Li}$ in state |1> is obtained in an optical dipole trap after sympathetic cooling with ${}^{23}\text{Na}$ in a magnetic trap. The equal (1, 3) mixture (that is, one containing the same number of atoms of each component) is prepared at 568 G, close to the zero crossing of a_{13} (the magnetic-field-dependent scattering length between atoms in states |1> and |3>). Here a non-adiabatic Landau–Zener radio-frequency sweep, creating an equal (1, 2) mixture, is followed by an adiabatic Landau–Zener sweep that transfers the atoms in state |2> to state |3>. To induce strong interactions, the magnetic field is adjusted in 100 ms to 730 G and then ramped to values between 660 and 833 G. After evaporative cooling in the optical trap, superfluidity is indirectly established by the observation of fermion pair condensates^{27,28}. Under comparable conditions, quantized vortex lattices—a certain indicator of superfluidity—have been observed in the rotating (1, 2) mixture of ${}^6\text{Li}$ (ref. 4). $E_F = h(v_r^2 v_{ax})^{1/3} (3N)^{1/3}$, with radial trapping frequency $v_r = 140 \text{ Hz}$, axial trapping frequency $v_{ax} = 22 \text{ Hz}$ and $k_F = \sqrt{2mE_F}/h$. The temperature T/T_F was determined from the shape of the expanded cloud.

Recording the (1, 3) radio-frequency spectra. The radio-frequency dissociation spectra at 670, 691, and 710 G are obtained by applying a 200- μs radio-frequency pulse to the (1, 3) mixture and monitoring the atoms transferred to state |2>. Three-dimensional image reconstruction by means of inverse Abel transformation is used to obtain local radio-frequency spectra⁸. The pulse length is chosen to be shorter than one-quarter the trapping period to minimize atomic diffusion during the excitation pulse. The radio-frequency power is adjusted to transfer fewer than 5% of the total number of atoms. A further reduction of the radio-frequency power affects the signal-to-noise ratio but not the spectral width. The bound–bound spectra and spectra at fields at and above 750 G are not spatially resolved, and are obtained using ~ 1 -ms pulses.

Full Methods and any associated references are available in the online version of the paper at www.nature.com/nature.

Received 3 February; accepted 17 June 2008.

- Eagles, D. M. Possible pairing without superconductivity at low carrier concentrations in bulk and thin-film superconducting semiconductors. *Phys. Rev.* **186**, 456–463 (1969).
- Leggett, A. J. in *Modern Trends in the Theory of Condensed Matter (Proc. 16th Karpacz Winter School Theor. Phys.)* (eds Pekalski, A. & Przystawa, J.) 13–27 (Springer, 1980).
- Nozières, P. & Schmitt-Rink, S. Bose condensation in an attractive fermion gas: from weak to strong coupling superconductivity. *J. Low Temp. Phys.* **59**, 195–211 (1985).
- Zwierlein, M. W., Abo-Shaeer, J. R., Schirotzek, A., Schunck, C. H. & Ketterle, W. Vortices and superfluidity in a strongly interacting Fermi gas. *Nature* **435**, 1047–1051 (2005).
- Ketterle, W. & Zwierlein, M. W. in *Ultra-Cold Fermi Gases (Proc. Internat. School Phys. ‘Enrico Fermi’, Course 164)* (eds Inguscio, M., Ketterle, W. & Salomon, C.) 95–287 (IOS Press, 2008).
- Chin, C. *et al.* Observation of the pairing gap in a strongly interacting Fermi gas. *Science* **305**, 1128–1130 (2004).
- Schunck, C. H., Shin, Y., Schirotzek, A., Zwierlein, M. W. & Ketterle, W. Pairing without superfluidity: The ground state of an imbalanced Fermi mixture. *Science* **316**, 867–870 (2007).
- Shin, Y., Schunck, C. H., Schirotzek, A. & Ketterle, W. Tomographic rf spectroscopy of a trapped Fermi gas at unitarity. *Phys. Rev. Lett.* **99**, 090403 (2007).
- Pistolesi, F. & Strinati, G. C. Evolution from BCS superconductivity to Bose condensation: Role of the parameter $k_F \xi$. *Phys. Rev. B* **49**, 6356–6359 (1994).
- Regal, C. A., Ticknor, C., Bohn, J. L. & Jin, D. S. Creation of ultracold molecules from a Fermi gas of atoms. *Nature* **424**, 47–50 (2003).
- Diener, R. B. & Ho, T.-L. The condition for universality at resonance and direct measurement of pair wavefunctions using rf spectroscopy. Preprint at (<http://xxx.tau.ac.il/abs/cond-mat/0405174>) (2004).
- Yu, Z. & Baym, G. Spin-correlation functions in ultracold paired atomic-fermion systems: Sum rules, self-consistent approximations, and mean fields. *Phys. Rev. A* **73**, 063601 (2006).

13. Baym, G., Pethick, C. J., Yu, Z. & Zwierlein, M. W. Coherence and clock shifts in ultracold Fermi gases with resonant interactions. *Phys. Rev. Lett.* **99**, 190407 (2007).
14. Punk, M. & Zwerger, W. Theory of rf-spectroscopy of strongly interacting fermions. *Phys. Rev. Lett.* **99**, 170404 (2007).
15. Perali, A., Pieri, P. & Strinati, G. C. Competition between final-state and pairing-gap effects in the radio-frequency spectra of ultracold Fermi atoms. *Phys. Rev. Lett.* **100**, 010402 (2008).
16. Gupta, S. *et al.* Rf spectroscopy of ultracold fermions. *Science* **300**, 1723–1726 (2003).
17. Bartenstein, M. *et al.* Precise determination of ^6Li cold collision parameters by radio-frequency spectroscopy on weakly bound molecules. *Phys. Rev. Lett.* **94**, 103201 (2005).
18. Regal, C. A. & Jin, D. S. Measurement of positive and negative scattering lengths in a Fermi gas of atoms. *Phys. Rev. Lett.* **90**, 230404 (2003).
19. Ortiz, G. & Dukelsky, J. BCS-to-BEC crossover from the exact BCS solution. *Phys. Rev. A* **72**, 043611 (2005).
20. Engelbrecht, J. R., Randeria, M. & Sá de Melo, C. A. R. BCS to Bose crossover: Broken-symmetry state. *Phys. Rev. B* **55**, 15153–15156 (1997).
21. Burovski, E., Prokof'ev, N., Svistunov, B. & Troyer, M. Critical temperature and thermodynamics of attractive fermions at unitarity. *Phys. Rev. Lett.* **96**, 160402 (2006).
22. Carlson, J., Chang, S.-Y., Pandharipande, V. R. & Schmidt, K. E. Superfluid Fermi gases with large scattering length. *Phys. Rev. Lett.* **91**, 050401 (2003).
23. Basu, S. & Mueller, E. J. Final-state effects in the radio frequency spectrum of strongly interacting fermions. Preprint at (<http://xxx.tau.ac.il/abs/0712.1007v2>) (2007).
24. Kinnunen, J., Rodríguez, M. & Törmä, P. Pairing gap and in-gap excitations in trapped fermionic superfluids. *Science* **305**, 1131–1133 (2004).
25. Ohashi, Y. & Griffin, A. Single-particle excitations in a trapped gas of Fermi atoms in the BCS-BEC crossover region. II. Broad Feshbach resonance. *Phys. Rev. A* **72**, 063606 (2005).
26. He, Y., Chen, Q. & Levin, K. Radio-frequency spectroscopy and the pairing gap in trapped Fermi gases. *Phys. Rev. A* **72**, 011602 (2005).
27. Regal, C. A., Greiner, M. & Jin, D. S. Observation of resonance condensation of fermionic atom pairs. *Phys. Rev. Lett.* **92**, 040403 (2004).
28. Zwierlein, M. W. *et al.* Condensation of pairs of fermionic atoms near a Feshbach resonance. *Phys. Rev. Lett.* **92**, 120403 (2004).
29. Honerkamp, C. & Hofstetter, W. Ultracold fermions and the SU(N) Hubbard model. *Phys. Rev. Lett.* **92**, 170403 (2004).
30. Chin, C. & Julienne, P. S. Radio-frequency transitions on weakly bound ultracold molecules. *Phys. Rev. A* **71**, 012713 (2005).

Supplementary Information is linked to the online version of the paper at www.nature.com/nature.

Acknowledgements We thank M. Zwierlein, W. Zwerger, E. Mueller and S. Basu for discussions and A. Keshet for the experiment control software. This work was supported by the NSF and ONR, through a MURI program, and under ARO Award W911NF-07-1-0493 with funds from the DARPA OLE programme.

Author Information Reprints and permissions information is available at www.nature.com/reprints. Correspondence and requests for materials should be addressed to C.H.S. (chs@mit.edu).

METHODS

Creation of new superfluid spin mixtures for radio-frequency spectroscopy.

For the well-established (1, 2) mixture, only the $|2\rangle$ -to- $|3\rangle$ transition has been used for radio-frequency spectroscopy. The final state s -wave scattering length a_{13} at B_{12} is large and negative, leading to strong final-state interactions with $1/k_F a_f < -1$ ($a_{13} \approx -3,300a_0$, where a_{ij} is the magnetic-field-dependent scattering length between atoms in states $|i\rangle$ and $|j\rangle$ and a_0 is the Bohr radius). The strength of the final-state interactions can in principle be changed in several ways without affecting the initial state. The density could be lowered to reduce the interaction strength in the final state while the initial state remains resonantly interacting. It is, however, experimentally difficult to decrease the density by a large factor and maintain the same low temperature T/T_F . We might also try spectroscopically to access a different final state. However, in ${}^6\text{Li}$ there are no other allowed transitions insensitive to the magnetic field. Magnetic field insensitivity is necessary to obtain the required spectral resolution in the kilohertz regime.

Because other mixtures of hyperfine states in ${}^6\text{Li}$ also exhibit broad Feshbach resonances, we attempt to create resonantly interacting superfluids in new combinations of initial hyperfine states: (1, 3) and (2, 3). The lifetimes of these spin mixtures at resonance exceed 10 s, implying inelastic collision rates smaller than $10^{-14} \text{ cm}^{-3} \text{ s}^{-1}$. For the (2, 3) superfluid the final-state interactions are also large and negative, but the final-state scattering length at B_{13} is either $a_{23} \approx 1,140a_0$ or $a_{12} \approx 1,450a_0$ (depending on the radio-frequency transition employed), and therefore considerably smaller and positive.

Creation of the (2, 3) superfluid. To prepare a (2, 3) superfluid, we follow essentially the same procedure as previously described for the (1, 2) mixture^{4,5}. The only difference is that instead of applying a Landau–Zener transfer that creates an equal (1, 2) mixture, a complete transfer to state $|2\rangle$ is followed by a second sweep, creating an equal (2, 3) mixture. The final magnetic field at the centre of the (2, 3) resonance is $B_{23} \approx 811 \text{ G}$. As in the other spin mixtures, we observe fermion pair condensation after evaporation in the optical trap.

Recording the (1, 3) spectra: stability of the mixture after the radio-frequency pulse. Recording the atoms transferred to state $|2\rangle$ is advantageous because there is no background without a radio-frequency pulse, but it requires that their lifetime with respect to three-body recombination be sufficiently long.

For fields below $\sim 710 \text{ G}$, we find that the lifetime of the $|2\rangle$ atoms after the radio-frequency pulse is short when they form a molecule with a $|1\rangle$ atom as the result of a bound–bound transition. Therefore, in some cases, the bound–bound parts of the spectra are recorded by observing atom number loss in the initial state. After bound–free excitation, the lifetime of atoms in state $|2\rangle$ is 30 ms (determined at 691 G), which is sufficiently long to observe the atoms directly. As a result of the different decay times and recording methods, the relative signal strength of the bound–bound and bound–free parts of the spectrum cannot be determined.

At fields above $\sim 750 \text{ G}$, we find similar and strong losses after both bound–free and bound–bound excitations. Therefore, all data are taken by monitoring losses in the initial state $|3\rangle$ and the spectra reflect the relative strength of bound–bound and bound–free transitions.

Fitting the (1, 3) spectra. The fit to the radio-frequency dissociation spectra in Figs 2, 3 and 4a–c uses a generic, model-independent pair dissociation line shape based on I_m with an additional parameter E_{offset} : $I_{\text{generic}}(E) \propto \sqrt{E - E_{\text{th}}}/(E - E_{\text{offset}})^2$. This line shape provides an excellent fit to simulated radio-frequency dissociation spectra both in the BEC and the BCS limit⁵ (see Supplementary Fig. 2). We used this line shape, convolved with the Fourier transform of the square pulses, as a fitting function, and found good agreement with the experimentally obtained spectra shown in Fig. 2. The generic fit function contains no corrections for final-state interactions. In the BEC limit (where $E_{\text{offset}} = 0$ and $E_{\text{th}} = E_b$), such corrections can be included³⁰ in a multiplicative factor of $1/(E + \hbar^2/m a_f^2 - E_{\text{th}})$. When applied to the dissociation spectra in the crossover, this correction factor changes the fit by only a negligible amount. All bound–bound spectra and the bound–free spectra in Fig. 4d–f have been fit using a Gaussian.

(1, 3) mixture: $|3\rangle$ -to- $|2\rangle$ versus $|1\rangle$ -to- $|2\rangle$ transition. The (1, 3) superfluid gives us the opportunity to record two different (magnetic-field-insensitive) radio-frequency spectra: from state $|3\rangle$ to state $|2\rangle$ (the transition used for all the spectra shown in the paper) and from state $|1\rangle$ to state $|2\rangle$. This allows us to compare radio-frequency spectra of the same system but for somewhat different final-state interactions. The final-state scattering lengths at B_{13} are $a_{23} \approx 1,140a_0$ for the $|1\rangle$ -to- $|2\rangle$ transition and $a_{12} \approx 1,450a_0$ for the $|3\rangle$ -to- $|2\rangle$ transition. Supplementary Fig. 1 shows the spectra at 691 G. Note that the fermion pair size obtained from the spectra agrees for both radio-frequency transitions, within the experimental uncertainty.